مجلة جامعة الزاوية للعلوم الطبيعية
University of Zawia Journal of Natural Sciences *(UZJNS)*
https://journals.zu.edu.ly/index.php/UZJNS ISSN: 3078-4999

Monte Carlo Modelling and Simulation of Gamma-Ray Dose Rates from Selected Radioactive Sources

Amena M Khamaj[a], Suad M Khamaj[a]

[a]*Department of Physics, Faculty of Sciences, University of Zawia, Zawia, Libya.*

*Corresponding *email address:* a.khamaj@zu.edu.ly

Received 06 Feb 2026 | Accepted 24 Mar 2026 | Available online 25 Mar 2026 | DOI: 10.26629/uzjns.2026.02

A B S T R A C T

This study presents a comprehensive investigation of external gamma-ray dose rates from Cs-137, Co-60, and Ir-192 sources, considering variations in source-to-detector distance and lead shielding thickness using Monte Carlo simulations with the GEANT4 toolkit. Dose rates were evaluated for two activity levels, 5MBq representing standard operational conditions and 10 MBq for model validation, at three distances (0.5 m, 1.5 m, and 3 m) and four lead thicknesses (0, 1, 2, and 5 cm). The results show a systematic decrease in dose rate with increasing distance, consistent with the inverse square law, and an exponential reduction with increasing lead thickness, reflecting photon attenuation within the shielding material. Energy-dependent attenuation effects were observed, with lower-energy photons from Cs-137 experiencing more effective reduction compared to higher-energy photons from C0-60, while Ir-192 exhibited intermediate attenuation characteristics, highlighting the influence of photon energy on shielding efficiency. Across identical geometrical configurations and activity levels, Co-60 produced the highest dose rates, followed by Ir-192, and then Cs-137, indicating a direct correlation between photon energy and external dose magnitude. The consistency of distance-dependent and thickness-dependent trends confirms the physical accuracy and computational reliability of the GEANT4-based Monte Carlo model. These findings provide a quantitative basis for optimizing shielding design, defining safe operational distances, and implementing effective radiation protection strategies in medical, industrial, and research environments in accordance with international safety standards. Furthermore, the study demonstrates that Monte Carlo simulations serve as a high-fidelity predictive tool for evidence-based radiological safety planning, supporting both practical applications and future research developments in complex radiological scenarios.

***Keywords**: Monte Carlo simulation, gamma-ray dosimetry, dose rates, lead shielding, radiation protection.*

النمذجة والمحاكاة بطريقة مونتي كارلو لمعدلات جرعة أشعة جاما المنبعثة من مصادر مشعة مختارة

أمينة خماج[a]، سعاد خماج[a]

[a]*قسم الفيزياء، كلية العلوم، جامعة الزاوية، الزاوية، ليبيا*

الملخص

تقدم هذه الدراسة تقييما علميا شاملا لمعدلات الجرعة الإشعاعية الخارجية لأشعة جاما المنبعثة من مصادر السيزيوم-137 (Cs-137) والكوبالت-60 (C0-60) والإريديوم-192(Ir-192) ، مع دراسة تأثير كل من المسافة بين المصدر والكاشف وسماكة التدريع الرصاصي، وذلك باستخدام محاكاة مونتي كارلو عبر حزمة GEANT4. تم تقييم معدلات الجرعة عند مستويي نشاط إشعاعي 5 ميغا بيكريل لتمثيل الظروف التشغيلية الاعتيادية و10 ميغا بيكريل للتحقق من صحة النموذج الحسابي، وعلى ثلاث مسافات (0.5 م، 1.5 م، و3 م)، وأربع سماكات لتدريع الرصاص (0، 1، 2، و5 سم). أظهرت النتائج انخفاضا متدرجا في معدلات الجرعة مع زيادة المسافة، بما يتوافق مع قانون التربيع العكسي، إضافة إلى انخفاض أسي مع زيادة سماكة الرصاص، وهو ما يعكس توهين الفوتونات داخل مادة التدريع. كما لوحظت تأثيرات التوهين المعتمد على الطاقة، حيث خضعت فوتونات الطاقة المنخفضة الصادرة عن السيزيوم Cs-137 لتوهين أكثر فاعلية مقارنة بفوتونات الطاقة الأعلى الصادرة عن الكوبالت Co-60، في حين أظهر الإريديوم Ir-192 خصائص توهين متوسطة، مما يبرز الدور الحاسم لطاقة الفوتونات في كفاءة التدريع. وعند نفس التكوينات الهندسية ومستويات النشاط الإشعاعي، سجل مصدر C0-60 أعلى معدلات الجرعة، تلاه Ir-192 ثم Cs -137، بما يشير إلى وجود علاقة مباشرة بين طاقة الفوتونات ومقدار الجرعة الإشعاعية الخارجية. كما يؤكد اتساق الاتجاهات المرتبطة بالمسافة وسماكة التدريع الدقة الفيزيائية والموثوقية الحسابية لنموذج مونتي كارلو المعتمد على GEANT4. توفر هذه النتائج أساسا كميا علميا لتصميم التدريع الأمثل، وتحديد المسافات التشغيلية الآمنة، وتطبيق استراتيجيات فعالة للحماية الإشعاعية في البيئات الطبية والصناعية والبحثية بما يتوافق مع المعايير الدولية للسلامة. كما تظهر الدراسة أن محاكاة مونتي كارلو تمثل أداة تنبؤيه عالية الدقة للتخطيط المبني على الأدلة في مجال السلامة الإشعاعية، بما يدعم التطبيقات العملية والتطويرات البحثية المستقبلية في السيناريوهات الإشعاعية المعقدة.

***الكلمات المفتاحية:** محاكاة مونتي كارلو، قياس جرعات أشعة جاما، معدلات الجرعة، التدريع بالرصاص، الحماية الإشعاعية.*

1. Introduction

This section introduces the scientific context of the study, defines the research problem, and outlines the objectives and scope of the work within the framework of radiation protection and gamma-ray dosimetry.

1.1 Background and significance of gamma radiation

Gamma radiation is a high-energy form of ionizing radiation that is widely applied in both medical and industrial applications, including radiotherapy, radiation calibration, and industrial imaging. Common gamma-emitting radionuclides such as Cesium-137(Cs-137), Cobalt-60 (Co-60), and Iridium-192 (Ir-192) play an important role in these applications. Despite their extensive use, exposure to gamma radiation may pose potential hazards to human health and the environment. This makes accurate evaluation of dose rate distributions essential to ensure the safety of workers, patients, and the public.

In radiation protection studies, particular attention is given to understanding how the dose rate varies with distance from the radiation source and how shielding materials can be used to reduce unnecessary exposure [1], [2]. Evaluating dose distribution helps in designing effective shielding, optimizing operational protocols, and complying with international safety standards, including those established by the International Atomic Energy Agency (IAEA) and the International Commission on Radiological Protection (ICRP) and relevant dosimetrist reports issued by bodies such as the National Council on Radiation Protection and Measurements (NCRP) and the International Commission on Radiation Units and Measurements (ICRU) [1], [2], [3], [4] [5].

1.2 Physical basis and limitations of analytical descriptions

The spatial behaviour of radiation intensity emitted from an ideal point source is commonly described by the inverse square law, which predicts that radiation intensity decreases inversely with the square of the distance from the source. This relationship provides a useful theoretical framework; however, it is based on idealized assumptions that are rarely satisfied in practical environments. In realistic conditions, several physical factors influence the actual dose rate distribution, including photon scattering, attenuation within surrounding media, finite source geometry, and variation in the energy of emitted gamma photons. As a result, analytical descriptions alone may not adequately represent realistic radiation fields, particularly in complex or shielded configurations [6].

1.3 Monte Carlo simulation for dose evaluation

To overcome the limitations of purely analytical approaches, Monte Carlo simulation methods are widely employed for radiation transport and dose calculations. These methods rely on statistical modelling of particle trajectories and radiation-matter interactions, allowing a more realistic representation of physical processes. Among the available Monte Carlo toolkits, GEANT4 has been extensively used in radiation physics and medical physics studies due to its validation physics models for gamma-ray interactions, including the photoelectric effect, Compton scattering, and pair production. Previous investigations have demonstrated that GEANT4 simulations show good agreement with experimental measurements and are consistent with internationally accepted radiation protection standards [7], [8].

1.4 Objectives and scope of the study

The primary aim of the present study is to numerically investigate gamma-ray dose rates from selected radioactive sources using Monte Carlo simulations based on the GEANT4 toolkit. Specifically, the study seeks to evaluate the influence of source-to-detector distance and lead shielding thickness on gamma-ray dose rates for Cesium-137 (Cs-137), Cobalt-60 (Co-60), and Iridium-192 (Ir-192) sources, considering two activity levels, representing both standard operational conditions and validation scenarios for the computational model.

In addition, the study aims to analyse the effect of photon energy and spectral composition on dose distribution, taking into account the single-energy emission of Cs-137, the dual-energy emission of Co-60, and the multi-energy emission of Ir-192, to understand the role of photon energy on penetration capability and shielding efficiency. Finally, the study seeks to assess the agreement between the simulated dose rates, theoretical radiation transport models, and internationally accepted radiation protection standards and guidelines, including recommendations issued by the IAEA, ICRP,

NCRP, and ICRU, thereby providing a quantitative foundation for evidence-based radiation protection planning and shielding optimization.

In this context, based on the physical principles and limitations of analytical models outlined above, a numerical Monte Carlo simulation framework was adopted to enable accurate modelling of gamma-ray transport, dose formation, and shielding effects under realistic geometrical and material conditions.

2. Methodology

This section presents the methodology used to simulate and analyse external gamma-ray dose rates from the sources under study, including the computational framework, geometrical setup, and evaluation of shielding effects.

2.1 Study Design and Simulation Objectives

This study was designed to estimate the dose rate distribution around gamma-emitting sources in a model environment using Monte Carlo simulation implemented through the GEANT4 toolkit [7]. The simulation framework enables detailed modelling of photon transport and interaction processes, including Compton scattering, photoelectric absorption, and electron-positron pair production. This approach allows for a systematic investigation of the influence of photon energy, source-to-detector distance, and shielding thickness on dose rate distributions, while providing a quantitative comparison with theoretical expectations based on the inverse square law and international radiation protection recommendations issued by the IAEA and ICRP [1], [2].

2.2 Radioactive Sources and Photon Energies

Three radioactive gamma sources were selected to cover a broad range of photon energies commonly encountered in radiation protection applications. Cesium-137 (Cs-137) was modelled as a monoenergetic gamma emitter with a photon energy of 0.662 MeV. Cobalt-60 (C0-60) was considered as a dual-energy source emitting photons at 1.17 MeV and 1.33 MeV. Iridium-192 (Ir-192) was modelled with a multi-energy photon spectrum ranging from 0.31 MeV to 0.61 MeV. This selection enables a comprehensive assessment of the impact of photon energy and spectral characteristics on dose rate attenuation and scattering phenomena [9].

2.3 Nominal Source Activity

Two nominal activity values were assigned to each source, namely 5MBq and 10 MBq. The use of two activities ensures that any observed variations in dose rate are attributable to changes in distance, shielding thickness, or photon energy rather than to the activity itself. Moreover, this approach allows verification of the linear dependence of dose rate on activity and supports the assessment of statistical stability in the Monte Carlo calculations, ensuring that the resulting dose distribution characteristics of the simulated system [10].

2.4 Geometrical Model and Measurement Points

Each radioactive source was positioned at the origin of the coordinate system within a virtual air-filled volume representing the surrounding environment. Virtual detectors were placed radially at distances of 0.5 m, 1.5 m, and 3 m from the sources to measure dose rates at representative locations relevant to radiation protection scenarios. Lead shielding layers with thickness of 0 cm (no shielding), 1 cm, 2 cm, and 5 cm were introduced around the source to evaluate the attenuation of gamma radiation as a function of shielding thickness. The use of air as the surrounding medium in all configurations allows for an independent assessment of the effects of distance, photon energy, and shielding on dose rate behaviour.

2.5 Monte Carlo Simulation Framework Using GEANT4

The Monte Carlo simulations were performed using GEANT4, which simulates particle transport through matter by generating random particle histories based on fundamental interaction cross sections. In this study, photon tracks were generated from the source and followed until absorption or escape from the simulation geometry, with all interaction process recorded. The electromagnetic interactions were modelled using the Standard Electromagnetic physics List in GEANT4, which includes a comprehensive set of validated models for photoelectric absorption, Compton scattering, Rayleigh scattering, bremsstrahlung, and electron-positron pair production over a wide energy range relevant to radiation protection studies [7]. Photon initial properties, secondary particle generation, and interaction probabilities were controlled through GEANT4's built-in random number generators to ensure statistically unbiased event sampling. For each simulation scenario, at least 10^6 Histories were executed, where each History represents the complete transport of a single photon and may include multiple interaction Events. This number of Histories was selected in accordance with best practices reported in the literature, as it provides a balance between statistical accuracy and computational efficiency, while significantly reducing statistical fluctuations in the calculated dose rates [10].

2.6 Data Processing and Statistical Analysis

The GEANT4 simulation produced raw output data for each Event and History, including the energy deposited in each virtual detector. These raw data were systematically processed to obtain final dose rate values for every combination of source, photon energy, activity, distance, and shielding thickness. First, the energy deposited in each detector was accumulated for every History to account for all interactions occurring along each photon track. Subsequently, the total deposited energy was averaged over all Histories to obtain a mean deposited energy value for each detector and simulation scenario. The mean deposited energy was then converted into dose rate as

$$\dot{D} = \frac{E_{absorbed}}{m.\Delta t} \quad (1)$$

Where $E_{absorbed}$ represents the average absorbed energy in joules (J), m is the mass of the detector or surrounding medium in kilograms (kg), and Δt is the effective simulation time interval in seconds (s). In order to ensure the statistical reliability of the results, the standard deviation of the deposited energy was calculated for each detector and measurement point, allowing quantification of statistical uncertainties and verification of convergence with increasing number of Histories.

The resulting dose rate values were compared across the two activity levels (5 MBq and 10 MBq), the three source-to-detector distances (0.5 m, 1.5 m, 3 m), and the four lead shielding thicknesses (0, 1, 2, 5 cm). This comparative analysis enables verification of the expected linear dependence of dose rate on activity, as well as the physical influence of photon energy, distance, and shielding on dose attenuation. The processed results were organized into detailed tables for each radionuclide (Cs-137, Co-60, and Ir-192), and corresponding dose rate curves were generated to illustrate trends with distance and shielding thickness, thereby providing a comprehensive quantitative basis for further analysis and interpretation [9]-[11].

2.7 Dose Rate Characteristics, Shielding Effect, and the Inverse Square Law

The calculated dose rates were compared with the theoretical inverse square law, expressed as

$$\dot{D}\,(r) = \dot{D}\,(r_0)\left(\frac{r_0}{r}\right)^2 \quad (2)$$

Where $\dot{D}\,(r)$ is the dose rate at distance r, and $\dot{D}\,(r_0)$ is the reference dose rate at the reference distance r_0. Any deviation from this ideal behaviour was attributed to photon scattering in air and attenuation in the shielding material. The attenuation of gamma rays in lead was described by the exponential attenuation law,

$$I = I_0 e^{-\mu x} \quad (3)$$

Where I is the transmitted intensity, I_0 is the incident photon intensity, μ is the linear attenuation coefficient of lead, and x is the lead thickness. This relationship provides the theoretical framework for understanding the observed dose reductions due to shielding. The effectiveness of lead shielding was evaluated for thicknesses of 0, 1, 2, and 5 cm for each source and photon energy. The analysis highlights the stronger attenuation of lower-energy photons emitted by Cs-137, compared to the higher-energy photons from Co-60, demonstrating the combined influence of photon energy and shielding material on dose reduction [9], [11].

2.8 Linkage to International Radiation Protection Standards

The present study was designed in accordance with the recommendations of the IAEA and ICRP to ensure compliance with annual dose limits for both workers and the public. The source, energy, activity, and lead thickness were evaluated against the permissible limits of 20mSv/year for occupational exposure and 1mSv/year for members of the public [1], [2]. Measurements were conducted at radial distances of 0.5 m, 1.5 m, and 3.0 m, with lead shielding layers of 0, 1, 2, and 5 cm. Comparison of these simulated values with the reference limits allowed for assessing the effectiveness of shielding and distance in reducing exposure. In scenarios where dose rates exceeded the limits, such as at 0.5 m without shielding, it became evident that additional protective measures, including thicker lead layers or increased separation from the source, are required.

Furthermore, the analysis revealed that low-energy photons, such as those emitted by Cs-137, are attenuated more readily than high-energy photons from Co-60, highlighting the significance of photon energy in shielding design. The systematic evaluation of all scenarios using the inverse square law confirmed that deviations from the expected decay are indicative of scattering or shielding effects, while the dose reduction achieved by increasing lead thickness demonstrates the efficiency of shielding in practical applications. Overall, the simulation-based assessment provides quantitative evidence for ensuring that all measurement points remain within the safe radiation limits, thereby validating the geometrical model, the

Selected shielding thicknesses, and distances as effective measures for radiation protection [1], [2], [11]. Consequently, using the defined simulation geometry, source configurations, and material parameters, the Monte Carlo calculations were performed to generate quantitative dose rate data for different distances and shielding conditions, as presented in the following section.

3. Results

All reported dose rates are expressed in $\mu Sv/h$. The presented results in Tables 1-3 and Figures 1(a),1(b)-3(a), 3(b) summarize the simulated external gamma-ray dose rates for Cs-137, Co-60, and Ir-192 at an activity of 5 MBq, evaluated at three source-detector distances (0.5 m, 1.5 m, and 3 m) and four lead shielding thicknesses (0, 1, 2, and 5 cm). Under unshielded conditions (0 cm lead), all sources exhibit high dose rates at short distances, followed by a systematic decrease with increasing distance. At 0.5 m, the unshielded dose rates reach 8 $\mu Sv/h$ for Cs-137, 15 $\mu Sv/h$ for Co-60, and 11 $\mu Sv/h$ for Ir-192. At 3 m, these values decrease to 0.24 $\mu Sv/h$, 0.45 $\mu Sv/h$, and 0.33 $\mu Sv/h$, respectively,

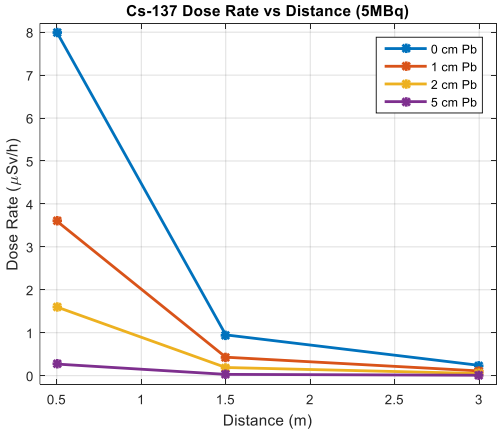

Figure 1(a). Cs-137 dose rate as a function of distance for different lead shielding thickness.

demonstrating a consistent distance-dependent reduction across all radionuclides.

The introduction of lead shielding produces a pronounced reduction in dose rates for all sources. Substantial attenuation is observed already at 1 cm thickness, with further reductions at 2 cm and 5 cm. At 5 cm lead thickness and 0.5 m distance, the dose rates are reduced to 0.27 $\mu Sv/h$ for Cs-137, 0.48 $\mu Sv/h$ for Co-60, and 0.35 $\mu Sv/h$ for Ir-192, confirming the effectiveness of lead shielding across different photon energy spectra.

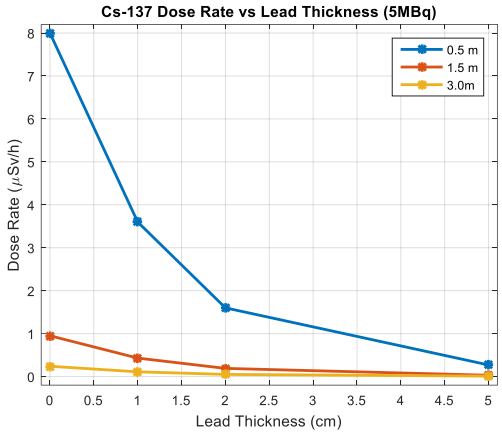

Figure 1(b). Cs-137 dose rate as a function of lead thickness at fixed source-detector distances.

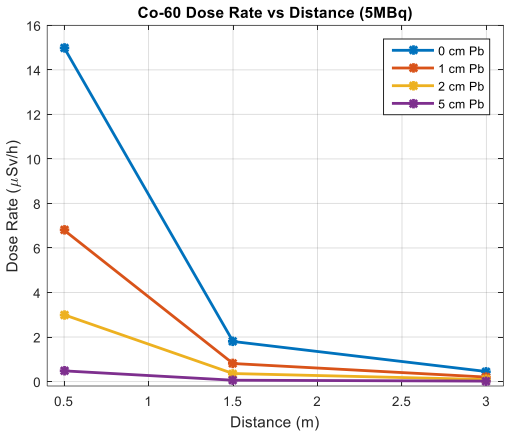

Figure 2(a). Co-60 dose rate as a function of distance for different lead shielding thickness.

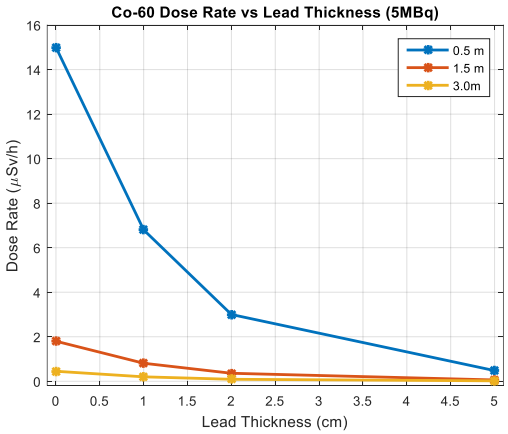

Figure 2(b). Co-60 dose rate as a function of lead thickness at fixed source-detector distances.

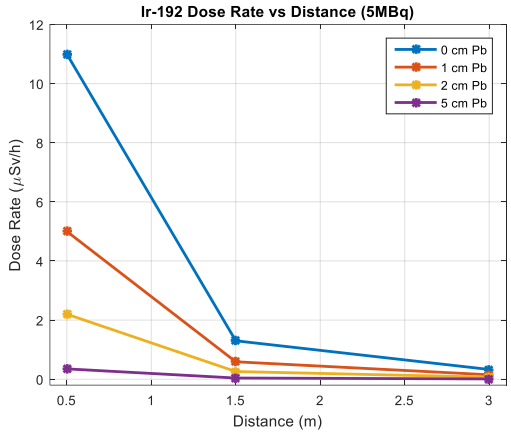

Figure 3(a). Ir-192 dose rate as a function of distance for different lead shielding thickness.

Figures 1-3 show consistent patterns for all sources: dose rates decrease monotonically with increasing distance for each fixed shielding thickness, and decrease with increasing lead thickness for each fixed distance. Panels (a) illustrate the distance-dependent dose curves for different shielding thicknesses, while panels (b) demonstrate the cumulative effect of lead thickness on dose rate at constant distances.

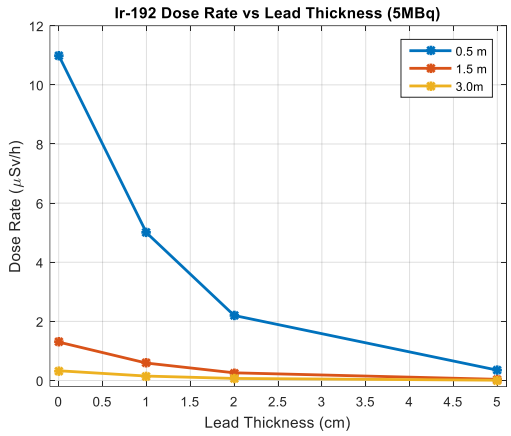

Figure 3(b). Ir-192 dose rate as a function of lead thickness at fixed source-detector distances.

Across identical geometrical configurations and activity levels, C0-60 consistently produces the highest dose rates, followed by Ir-192 and Cs-137. This relative dose ranking remains stable under both unshielded and shielded conditions across all distances and shielding configurations.

3.1 Source-Specific Observations

Cs-137: Shows the lowest dose rates under all geometrical and shielding configurations, with strong sensitivity to lead shielding, particularly at small thicknesses.

Co-60: Produces the highest dose rates across all distances and shielding conditions, reflecting its higher photon energies and greater penetration capability.

Ir-192: Exhibits intermediate dose levels and attenuation behaviour, consistent with its multi-energy photon spectrum and intermediate penetration characteristics.

For completeness and model validation, additional dose rate results for the 10 MBq activity level are provided in Appendix. These results reproduce the same spatial and shielding trends observed at 5MBq, confirming the linear activity scaling and numerical stability of the Monte Carlo simulations [1].

Accordingly, the simulated dose distributions and attenuation trends obtained from the Monte Carlo calculations are interpreted and analysed in the context of radiation transport physics, shielding theory, and energy-dependent interaction mechanisms in the following discussion.

Table 1 Monte Carlo-simulated external gamma-ray dose rates for Cs-137 (5MBq) as a function of source-detector distance and lead shielding thickness.

Thickness / Distance	*0 cm*	*1 cm*	*2 cm*	*5 cm*
0.5 m	8.0	3.6	1.6	0.27
1.5 m	0.95	0.43	0.19	0.03
3.0 m	0.24	0.11	0.05	0.01

.

Table 2 Monte Carlo-simulated external gamma-ray dose rates for Co-60 (5MBq) as a function of source-detector distance and lead shielding thickness

Thickness / Distance	*0 cm*	*1 cm*	*2 cm*	*5 cm*
0.5 m	15.0	6.8	3.0	0.48
1.5 m	1.8	0.81	0.63	0.06
3.0 m	0.45	0.20	0.09	0.02

Table 3 Monte Carlo-simulated external gamma-ray dose rates for Ir-192 (5MBq) as a function of source-detector distance and lead shielding thickness.

Thickness / Distance	*0 cm*	*1 cm*	*2 cm*	*5 cm*
0.5 m	11.0	5.0	2.2	0.35
1.5 m	1.30	0.59	0.26	0.04
3.0 m	0.33	0.15	0.07	0.01

4. Discussion

Following the presentation of the simulated dose rates in the Results section, it is clear that both

geometric and material factors play essential roles in shaping external gamma-ray dose fields from Cs-137, Co-60, and Ir-192 sources. The trends observed in Tables 1-3. and Figures 1(a),1(b)-3(a),3(b) highlight systematic variations of dose rates as functions of source-to-detector distance and lead shielding thickness, providing a quantitative basis for understanding the interplay between spatial dispersion, shielding effects, and photon energy.

4.1 Geometric Dispersion and Inverse Square Behaviour

The observed reduction in dose rate with increasing distance across all radionuclides is fundamentally governed by the inverse square law, which describes the spatial dilution of photon fluence from isotropic point sources [12]. For instance, Cs-137 without shielding (0 cm lead) exhibits a decrease from 8 $\mu Sv/h$ at 0.5 m to 0.24 $\mu Sv/h$ at 3 m as illustrated in Table 1 and Figure 1(a), demonstrating the dominate role of geometric dispersion at short separations. Similar unshielded trends are observed for Co-60 and Ir-192, with initial dose rates of $15\mu Sv/h$ and $11\mu Sv/h$ at 0.5 m, respectively, as shown in Tables 2,3 and Figures 2(a), 3(a). Steep photon fluence gradients at short distances become progressively more gradual at larger separations, reflecting classical geometric attenuation.

4.2 Shielding Attenuation Mechanisms

The application of lead shielding (1-5 cm) significantly modifies the dose profiles compared to the unshielded reference (0 cm). For example, at 0.5 m, Cs-137 dose decreases from 8 $\mu Sv/h$ without shielding to 3.6 $\mu Sv/h$ at 1 cm lead and further to $0.27\mu Sv/h$ at 5 cm as reported in Table 1 and noticed in Figure 1(b). Similarly, Co-60 and Ir-192exhibit pronounced reductions with increasing shielding thickness as can be seen in Tables 2, 3 and shown in Figures 2(b), 3(b), although the absolute decrease is moderated by photon energy. The rapid dose reduction at thinner shields is primarily due to photoelectric absorption and Compton scattering of primary photons, while the slower decline at thicker shields reflects contributions from scattered photons and secondary radiation, consistent with Monte Carlo transport models [13], [14].

4.3 Energy-Dependent Attenuation and Spectral Effects

Energy-dependent effects are clearly manifested in the simulations. Cs-137 photons (662 KeV) experience more effective attenuation under identical shielding compared to intermediate-energy Ir-192 photons (average energy spectrum around 380 KeV), whereas Co-60 photons (1173 and 1332 KeV) penetrate lead most efficiently as clearly illustrated in Tables 1-3 and shown in Figures 1(a), 1(b)-3(a),3(b). This hierarchy is reflected numerically across all tested thicknesses: Co-60 produces the highest dose rates, followed by Ir-192 and Cs-137, underscoring the influence of photon energy on shielding efficiency [15], [16]. Importantly, the 10 MBq simulations, presented in the Appendix as dose-distance and attenuation curves, reproduce the same physical trends observed at 5MBq, confirming that the higher activity level primarily serves to validate the computational model and linear dose-activity behaviour rather than alter the qualitative conclusions.

4.4 Combined Effects of Distance and Shielding on Dose Fields

The dose reduction arises from the coupled effects of geometric dispersion and material attenuation. At short distances, the presence of shielding exerts a dominant influence on dose reduction., whereas at longer distance, geometric dilution becomes more significant. For example, Cs-137 at 0.5 m decreases from 8 $\mu Sv/h$ unshielded to $0.27\mu Sv/h$ with 5 cm lead, while at 3 m the same shield reduces the dose from $0.24\mu Sv/h$ to $0.01\mu Sv/h$ as summarized in Table 1 and Figure 1(b). This multiplicative behaviour is observed consistently for C0-60 and Ir-192 as presented in Tables 2, 3 and observed in Figures 2(b), 3(b) corroborating previous Monte Carlo studies and supporting integrated radiation protection strategies [17].

4.5 Implications for Radiation Protection and Shielding Design:

From a radiation protection perspective, these results offer quantitative guidance for designing shielding systems. Lower-energy gamma sources achieve significant dose reduction with modest lead thicknesses, whereas higher-energy sources, such as Co-60, require thicker shields to reach comparable protection levels. These findings have direct relevance for facility design, radioactive source storage, medical physics installations, and industrial radiography systems, aligning with international radiation safety principles and shielding design frameworks [1].

4.6 Model Reliability and Computational Validity

The internal consistency between distance-dependent and thickness-dependent trends, the energy-dependent attenuation hierarchy, and the coherence of the dose distributions across all

radionuclides collectively validate the reliability of the Geant4-based Monte Carlo model. The correspondence between numerical values in the tables and the shapes of the curves in the figures confirms that the simulation framework accurately reproduces fundamental radiation transport physics, offering a high-fidelity predictive platform for dose assessment [13], [14], [17], [16]. Therefore, building on the physical interpretation and quantitative analysis of the simulation results, the main conclusions and practical implications of this study are summarized in the following section.

5. Conclusion

This study provides a comprehensive Monte Carlo-based assessment of external gamma-ray dose fields generated by Cs-137, C0-60, and Ir-192 sources under controlled variations in source-to-detector distance and lead shielding thickness. The results demonstrate that dose distribution is governed by a coupled physical mechanism combining geometric dispersion, described by the inverse square law, and material attenuation, governed by exponential photon interaction processes within the shielding medium. The systematic decrease in dose rate with increasing distance confirms the dominance of spatial photon fluence dilution, particularly under unshielded and weakly shielded conditions, while the exponential attenuation trends observed with increasing lead thickness reflect classical gamma attenuation physics. The simulations further reveal a clear energy-dependent attenuation behaviour, where photon energy directly controls penetrations capability and shielding efficiency. This is quantitatively reflected in the consistent ordering of dose magnitudes across all configurations, where C0-60 produces the highest dose rates, followed by Ir-192 and Cs-137, emphasizing the fundamental role of photon interaction cross-sections and mean free paths in dose formation. The internal consistency between distance-dependent trends, thickness-dependent attenuation patterns, and spectral energy effects confirms the physical validity of the Geant4-based Monte Carlo model and its ability to accurately reproduce fundamental radiation transport mechanisms.

The inclusion of dual activity levels demonstrates linear dose-activity behaviour, with the higher activity scenario serving primarily as a verification of computational stability and model reliability rather than altering the underlying physical trends. In addition, the obtained dose trends and attenuation behaviours are fully consistent with international radiation protection principles and shielding design recommendations issued by authoritative bodies such as the IAEA and the ICRP. The observed distance-dose relationships, shielding efficiency patterns, and energy-dependent attenuation mechanisms align with established international safety standards for external exposure control and radiological protection optimization frameworks, confirming the regulatory relevance and practical applicability of the simulation outcomes.

Collectively, these findings provide a quantitative and physically grounded framework for radiation protection analysis, supporting optimized shielding design, safe operational distance determination, and evidence-based radiological safety planning in medical, industrial, and research environments. The study therefore establishes Monte Carlo simulation as a high-fidelity predictive tool for integrated dose assessment and radiation protection system design, combining physical accuracy, computational reliability, and regulatory consistency within a unified radiological safety framework.

6. Future work

The results of this study open multiple research pathways for advancing quantitative dose modelling and radiation protection strategies based on numerical simulations. Future research may extend the Monte Carlo framework to include more realistic geometrical configurations representing medical, industrial, and research environments, such as radiotherapy rooms, nuclear medicine facilities, and radioactive source storage areas, enabling improved assessment of multiple scattering effects and secondary radiation contributions under realistic operational conditions. The investigation of multilayer shielding systems using composite materials, including lead-concrete and lead-polyethylene structures, offers a promising direction for optimizing attenuation efficiency while minimizing shielding mass.

Further developments may incorporate energy-resolved dosimetry analysis, fluence-to-effective dose conversion modelling, and uncertainty quantification frameworks to enhance the robustness and predictive reliability of dose calculations. Coupling numerical simulations with experimental validation using calibrated dosimetry measurements would provide critical verification for regulatory acceptance and practical implementation. Finally, the model may be applied in simulation-based decision support systems for radiation protection, supporting optimized determination of safe

operational distances, shielding requirements, and exposure management in both routine and emergency radiological scenarios.

7. Appendix

7.1 Dose Rates for 10 MBq Activity Level

The 10 MBq results confirm the Monte Carlo model's linear response to activity and validate the computational approach used for dose assessment. All curves in Figures A1-A6 at 10 MBq confirm the trends observed in the main text.

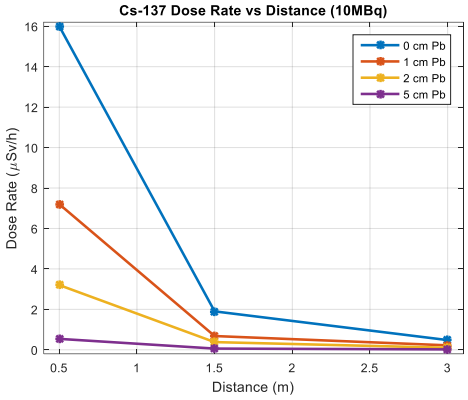

Figure A(1). Cs-137 dose rate as a function of distance for different lead shielding thickness.

.

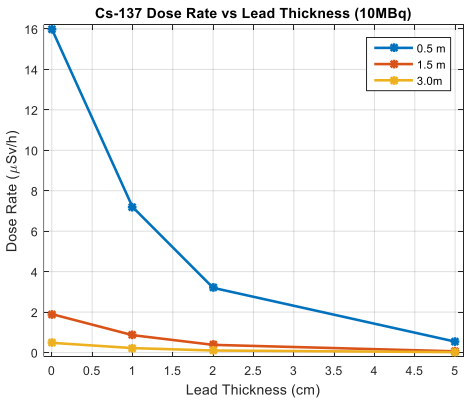

Figure A(2). Cs-137 dose rate as a function of lead thickness at fixed source-detector distances.

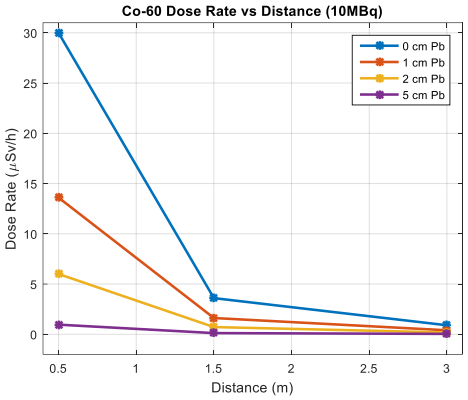

Figure A(3). Co-60 dose rate as a function of distance for different lead shielding thickness.

.

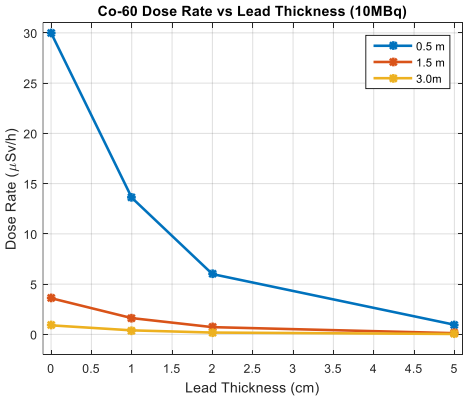

Figure A(4). Co-60 dose rate as a function of lead thickness at fixed source-detector distances.

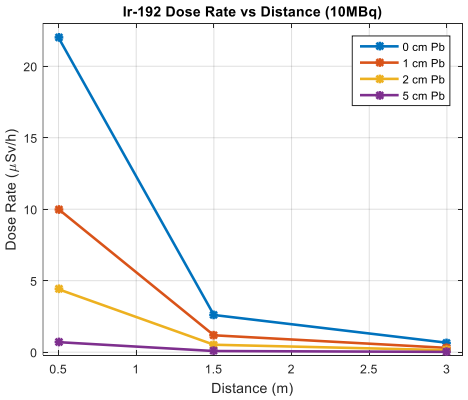

Figure A(5). Ir-192 dose rate as a function of distance for different lead shielding thickness.

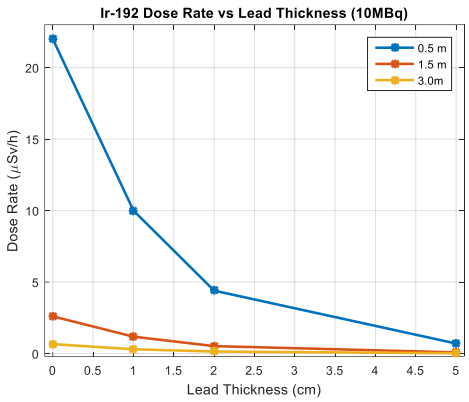

Figure A(6). Ir-192 dose rate as a function of lead thickness at fixed source-detector distances.

References

[1] International Atomic Energy Agency (IAEA), *Radiation protection and safety of Radiation Sources: International Basic safety standards*, Safety Standards Series No. GSR Part 3, Vienna, Austria: IAEA, 2014.

[2] J. Valentin, "The 2007 recommendations of the international commission on radiological protection," *ICRP publication*, vol. 103, pp. 2-4, 2008.

[3] International Commission on Radiation Units and Measurements (ICRU), *Operational Quantities for External Radiation Exposure*, ICRU Report 95, 2023.

[4] National Council on Radiation Protection and Measurements (NCRP), *Management of Exposure to Ionizing Radiation*. NCRP Report No. 180, 2018.

[5] National Council on Radiation Protection and Measurements (NCRP), *Limitation of exposure to ionizing radiation*. NCRP Report No. 116, 1993.

[6] J. R. Lamarsh and A. J. Baratta, *Introduction to nuclear engineering*. Pearson Education, Incorporated, 2018.

[7] S. Agostinelli, J. Allison, K.a. Amako, J. Apostolakis, H. Araujo, P. Arce, M. Asai, D. Axen, S. Banerjee and G. Barrand,"Geant4—a simulation toolkit," *Nuclear instruments and methods in physics research section A: ccelerators, Spectrometers, Detectors and ssociated Equipment*, vol. 506, no. 3, pp. 250-303, 2003.

[8] J. Allison, K. Amako, J. Apostolakis, P. Arce, M. Asai, T. Aso, E. Bagli, A. Bagulya, S. Banerjee, and G. Barrand, "Recent developments in Geant4," *Nuclear instruments and methods in physics research section A: Accelerators, Spectrometers, Detectors and Associated Equipment*, vol. 835, pp. 186-225, 2016.

[9] G. F. Knoll, *Radiation detection and measurement*. John Wiley & Sons, 2010.

[10] H .Özdoğan, Y. A. Üncü, F. Akman, H. Polat, and M. R. Kaçal, "Detailed analysis of gamma-shielding characteristics of ternary composites using experimental, theoretical and Monte Carlo simulation methods," *Polymers*, vol. 16, no. 13, p. 1778, 2024.

[11] D. S. Smith and M. G. Stabin, "Exposure rate constants and lead shielding values for over 1,100 radionuclides," *Health physics*, vol. 102, no. 3, pp. 271-291, 2012.

[12] International Commission on Radiation Units and Measurements (ICRU), *Fundamental Principles of Radiation Protection Dosimetry*, ICRU Report 85, 2019.

[13] M. J. Rivard, B. M. Coursey, L. A. DeWerd, W. F. Hanson, M. Saiful Huq, G. S. Ibbott, M. G. Mitch, R. Nath, and J. F. Williamson, "Update of AAPM Task Group No. 43 Report: A revised AAPM protocol for brachytherapy dose calculations," *Medical physics*, vol. 31, no. 3, pp. 633-674, 2004.

[14] T. Siiskonen, M. Tapiovaara, A. Kosunen, M. Lehtinen, and E. Vartiainen, "Monte Carlo simulations of occupational radiation doses in interventional radiology," *The British journal of radiology*, vol. 80, no. 954, pp. 460-468, 2007.

[15] S. M. B. Saleh, H. M. Albangahzi, and S. M. Alarabi, "Utilization of Geant4 Monte Carlo Code for Simulations of Gamma Ray Attenuation Coefficients in Selected Materials," *African Journal of Advanced Pure and Applied Sciences*, pp. 401-412, 2025

[16] K. Takahashi, “Photon interactions and energy-dependent attenuation in shielding materials,” *Radiation Physics and Chemistry*, vol. 179, p. 109281, 2021.

[17] J. F. Carrier, L. Archambault, L. Beaulieu, and R. Roy, "Validation of GEANT4, an object-oriented Monte Carlo toolkit, for simulations in medical physics," *Medical physics*, vol. 31, no. 3, pp. 484-492, 2004.